Modeling Biology – Structures, Behaviors, Evolution

Manfred D. Laublicher and Gerd B. Müller (eds)
The MIT Press 2007, Cambridge, Massachusetts

Chapter 10 – Modeling Neuronal Growth and Shape - pp 195-215

Jaap van Pelt, Harry B.M. Uylings
jaap.van.pelt@cncr.vu.nl; hbm.uylings@vumc.nl

(preprint)

Neurons are the cells of the nervous system involved in the processing of information. With their highly branched axons and dendrites they exchange electrical signals through a dense neuronal network of synaptic connections. Incoming electrical signals at an individual neuron are integrated by the dendritic trees and trigger this nerve cell to generate new electrical signals being relayed via the axonal processes to other neurons. The information processing characteristics of a neuron depend on this signal integration process, determined by the shape of dendrites and their electrophysiological properties (e.g., Mason and Larkman, 1990). Dendrites have a limited extension in space, while axons may run over long distances. Neurons appear in the nervous system with an enormous diversity in shapes, which is thought to contribute to their functional specialization. An illustration of this diversity is given in figure 10.1 showing dendritic shape differentiation in length scales and in the details of the branching patterns.

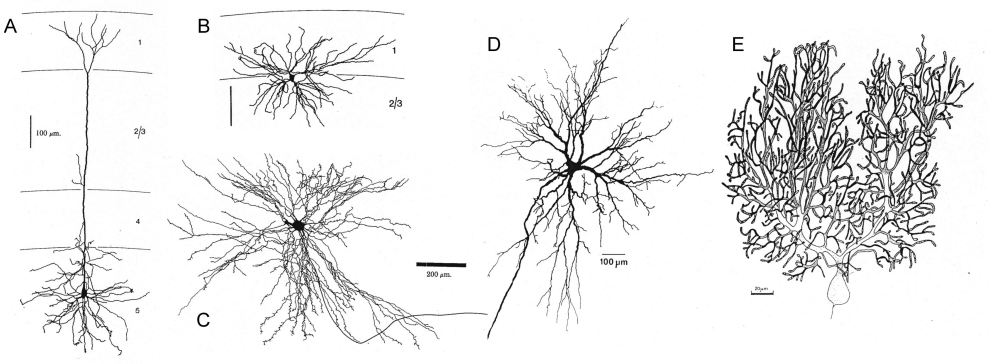

Figure 10.1
Neuronal branching patterns from different cell types in the nervous system, (A) rat cortical layer 5 pyramidal cells (adapted from Larkman and Mason, 1990), (B) rat cortical layer 2/3 pyramidal cells (adapted from Larkman and Mason, 1990), (C) newborn kitten α-motoneuron (adapted from Uhlfhake and Cullheim, 1988) , (D) cat deep superior colliculus neurons (adapted from Schierwagen and Grantyn, 1986, and Schierwagen, 1986) and (E) rat cerebellum Purkinje cell (adapted from Berry and Bradley, 1976a).

Neurons attain their shapes through a developmental process of elongation and branching of their axonal and dendritic extensions (collectively called neurites). Shape differentiation must therefore find its origin in the details of this developmental process. How shape characteristics of neurons reflect developmental information is nevertheless a question difficult to solve, not only because of the complexity of dendritic shapes but also of the dynamic process of dendritic development. Theoretical and computational modeling approaches are required for the quantification of dendritic shapes and for quantifying the developmental process through which these shapes emerge.

Modeling in Biology

In order to gain understanding of nervous system development and function, experimental work needs to be complemented by theoretical analysis and computer simulation. Even for biological systems in which all the components are known, computational models are necessary to explore and understand how the components interact to make the system work and how phenomena at different levels of organization or description are linked.

A model can be considered as a theoretical / computational tool to implement quantitatively knowledge and hypotheses about a system and enabling the study of the properties of that system. Modeling approaches depend strongly on the questions being raised (see also Leonelli, this volume). Knowledge and hypotheses are products of the human mind. They originate from human understanding of nature but need models for quantitative implementation. Nature is explored through human observations and is represented by quantitative data. Model validation of the experimental data provides the basis for obtaining understanding from the data, thereby bridging human mind and nature (figure 10.2).

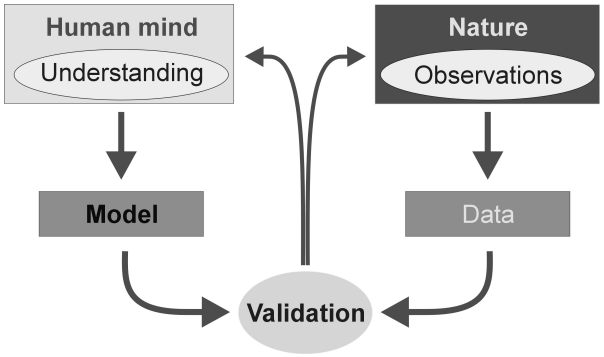

Figure 10.2
Role of a model as a tool to implement understanding from the human mind, to express hypotheses and to validate predictions against experimental data, originating from observations of nature.

Biological systems are complex at any level of their structural and functional organization, from the molecular up to the behavioural level. They consequently represent systems of (almost) infinite dimensionality. Building models of biological systems thus requires a well-thought approach to reduce this dimensionality to a meaningful and treatable level. Starting with a focus on selected mechanisms or phenomena, the level of dimensional reduction strongly depends on the particular research question and may range from the most reductionistic 'conceptual' models to complex but still computational treatable models. For instance, a typical method to reduce dimensionality is the statistical one in which the many degrees of freedom are lumped into a single probability function and the system is regarded as stochastic (Monte-Carlo approach). Other modeling approaches may preferably integrate all available knowledge aiming at studying the fine structure of the systems behavior. Biophysical models aim at understanding a well-defined system from the underlying biophysical laws of nature.

Biological systems distinguish themselves from physical systems in that they show organization at all levels of spatial and temporal scales, apparent for instance in genetic regulation of protein synthesis at the molecular level, and in feedback, homeostatic and adaptive mechanisms throughout the organism. Of course, biological systems are subjected to (bio)physical constraints which, for instance, becomes apparent when conservation laws result in limiting resources and competitive phenomena.

Biology of Neurite Outgrowth and Neuronal Morphogenesis

Neurite Outgrowth and Branching

Neurons grow out by a process of elongation and branching of their neuritic extensions. These processes are governed by the dynamic behavior of *growth cones*, highly motile structures at the tips of outgrowing neurites. Neurite elongation requires the polymerization of tubulin into cytoskeletal microtubules. Branching occurs when a growth cone, including its actin cytoskeletal meshwork, splits in two parts while partitioning the number of microtubules, and each daughter growth cone continuing to grow on their own (e.g., Black (1994); Kater et al., (1994); Kater and Rehder, (1995); Letourneau et al., (1994). Growth cones may also retract by microtubule depolymerization, or may redirect their orientations. The dynamic behavior of a growth cone results from the integrated outcome of many intracellular mechanisms and interactions with its local environment. These include, for instance, the exploratory interactions of its filopodia with a variety of extracellular (e.g., guidance, chemorepellant, chemoattractant) molecules in the local environment (e.g. Kater et al., 1994, McAllister, 2002; Whitford et al., 2002), receptor mediated trans-membrane signaling to cytoplasmic regulatory systems (e.g. Letourneau et al., 1994), intracellular regulatory genetic and molecular signaling pathways (e.g., Song and Poo, 2001), and electrical activity (e.g., Cline, 1999; Ramakers et al., 1998, 2001; Zhang and Poo, 2001).

Microtubule Cytoskeleton

In addition to regulatory mechanisms, dendritic outgrowth is also subjected to constraints, limiting their modulatory responsiveness. For instance, neurite elongation proceeds by growing mitrotubules, which requires the production, transport and polymerization of tubulin cytoskeletal elements. The production rate of cytoskeletal elements will set an upper limit to the averaged total length increase of the dendrite. In addition, the division of flow of cytoskeletal elements at a bifurcation will modulate the elongation rate of the daughter branches. Earlier model studies of microtubule polymerization (neurite elongation) in relation to tubulin production and transport demonstrated how limited supply conditions may lead to competition between growth cones for tubulin, resulting in alternating advance and immobilization (Van Ooyen, 2001). Empirical evidence for such competitive behavior has subsequently been obtained from time-lapse studies of outgrowing neurons in tissue culture by Ramakers (see Costa et al., 2002).

Synapse Stabilization

Limiting resources may also lead to competitive phenomena between axons, where target derived neurotrophins are required for the maintenance and stabilization of synaptic axonal endings on target dendrites. Modeling studies have shown that the precise manner in which neurotrophins regulate the growth of axons determines what patterns of target innervation can develop (Van Ooyen and Willshaw, 1999). Taking a spatial dimension into account these authors show that the distance between axonal endings on the target dendritic tree mitigates competition and permits the coexistence of axons (Van Ooyen and Willshaw, 2000). These examples just illustrate the complexity of the outgrowth process in terms of involved molecules, interactions, signaling pathways and constraints.

The integrated action and the details of all these intracellular and extracellular mechanisms will finally form the basis of dendritic morphological characteristics, of morphological differentiation between cell types and the diversity between neurons of the same type (e.g., Acebus and Ferrus, 2000).

Modeling Neuronal Shape

The complexity of dendritic shape has already for a long time been a challenge to computational modelers to extract regularities or common features and to synthesize realistic structures. Present studies show high levels of sophistication in the realism of reconstruction of dendritic trees including also the 3D orientation of branches and environmental influences (e.g., Ascoli et al., 2001; Ascoli 2002a,b; Samsonovich and Ascoli, this Volume). An

analytical approach was used by Kliemann (1987), Carriquiry et al., (1991) and Uemura et al. (1995) who considered the segments at a given centrifugal order as individuals of a generation, which may give rise to individuals in a next generation (i.e., by producing a bifurcation point with two daughter segments). Mathematically, such a dendritic reconstruction could be described by a Galton-Watson process, based on empirically obtained splitting probabilities for defining per generation whether or not a segment will be a terminal or an intermediate one. Tamori (1993) used a set of six 'fundamental parameters' to describe dendritic morphology, and analyzed branch angles using a principle of least effective volume. Growth models have been applied by e.g., Smit et al., 1972; Berry and Bradley, 1976b; Van Pelt and Verwer, 1983, Ireland et al., 1985, Horsfield et al., 1987 and Nowakowski et al., 1992. The growth model reviewed in this chapter is developed to answer the question whether morphological details and variability observed in dendritic branching patterns can be understood quantitatively in terms of a minimal set of growth rules.

Parametrization of Dendritic Shape

A first step requires the parametrization of dendritic shape, i.e. the reduction of morphological complexity into a set of well-defined shape parameters. Dendritic shape can be quantified in terms of the number of branch points, number of segments, length of segments, the connectivity pattern of segments (topological structure), segment diameters, curvature of segments and embedding in 3D space. Experimentally reconstructed dendrites show characteristics and variability in all these measures (e.g., Ascoli et al., 2001, Uylings and Van Pelt, 2002; Scorcioni et al., 2004; Samsonovich and Ascoli, this Volume), which require modeling studies to make specific choices on shape parameters to investigate.

Assumptions and Structure of the Model

The second step is to develop the model structure on the basis of well-defined assumptions. In our approach dendrites are described as binary rooted trees. Intermediate and terminal segments are distinguished and labeled with a centrifugal order indicating the number of segments on the path from the root to the segment. As discussed above dendrites develop from initial protrusions from the cell body into branched and elongated structures through dynamic actions of growth cones. Although these actions may include forward migration and branching but also retraction or complete disappearance, at a sufficient coarse time scale the net outcome is still a growing dendrite with increasing length and number of branches, as is schematically illustrated in figure 10.3.

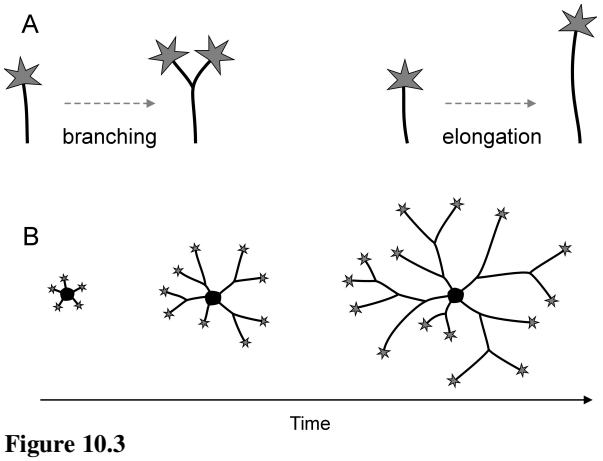

Figure 10.3

(A) Basic actions of a growth cone, splitting of a growth cone resulting in neurite branching, and migration of a growth cone, resulting in neuritic elongation, (B) Schematic illustration of the branching and elongation process mediated by growth cones. Initial protrusions from the cell body develop into mature dendritic trees through a process of growth cone elongation and branching.

In the model description a phenomenological approach is used in which not the intra- and extracellular mechanisms and processes are modeled themselves but their final outcome. To this end, the detailed dynamic actions of outgrowing neurites are coarse-grained and modeled by sustained processes of elongation and branching. The multitude of mechanisms involved in growth cone behavior (see previous section) justifies a stochastic description in which terminal segments elongate and branch with given probabilities per unit of time. These elongation and branching probability functions form the basic components of the model. The challenge is to find minimal but sufficient expressions for these functions to describe morphological characteristics and variability. When successful, these functions reflect important biological properties in the development of neuronal morphology. Branching and elongation are assumed to be independent making it possible to study both processes separately.

Variation in Topological Tree Types

To study the variation in the connectivity pattern of segments, dendrites will be reduced to binary tree types, ignoring any metrical property, as is illustrated in figure 10.4. Only a finite number of tree types are possible for a given number of segments. A branching event in a given tree increases its number of branch points and segments with one. Dependent on the branching segment, the given tree transforms into one of the tree types in the next row in figure 10.4. Not all transitions are possible between tree types at successive rows. The dashed arrows in figure 10.4A denote all possible transitions when branching is allowed at any segment in a tree. When branching is restricted to terminal segments only (as in the dendritic growth model), this will further reduce the number of possible transitions (figure 10.4B).

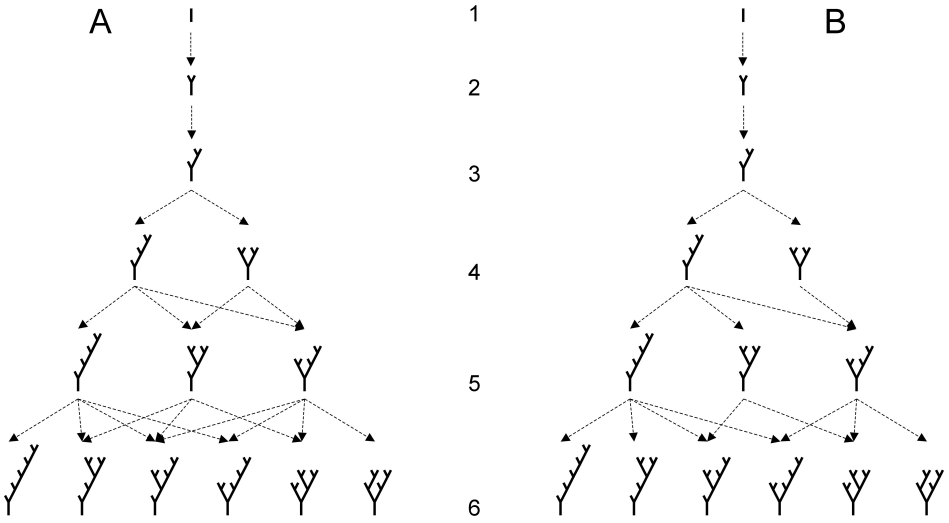

Figure 10.4
Possible transitions between topological tree types by branching of (A) any of the segments in the tree, or (B) of one of the terminal segments only.

In the stochastic branching process, each segment in a tree has a given probability to be selected for branching, which will add to the probability of the transition of that tree to one of its successors (outgoing dashed arrows for a given tree type in figure 10.4). The figure illustrates that different paths starting from the single segment may end in a particular tree type. A given number of branching events will result in one of the trees at a row (with a number of terminal segments equal to one plus the number of branching events). The probability that a given tree type is obtained thus results from the probabilities of all the possible paths, and thus of all the transitions (growth steps) in these paths. Both the number of possible paths and the probability of each growth step depend on the specific rules for branching of the individual segments in the branching tree. The eventual probability

distribution of tree types can be obtained by enumerating all the growth paths and their associated probabilities.

In a series of studies these probabilities have been calculated for a number of branching rules, i.e. (i) random segmental branching when each segment has the same probability to be selected for branching, (ii) random terminal branching when only terminal segments can be selected for branching with equal probabilities, and (iii) a branching scheme where the probability of branching is modulated by the position of the segment in the tree (e.g., Van Pelt and Verwer, 1986). These studies have demonstrated how the topological variation between tree types depends on the specific rules for branching of the individual segments (e.g., figure 10.5).

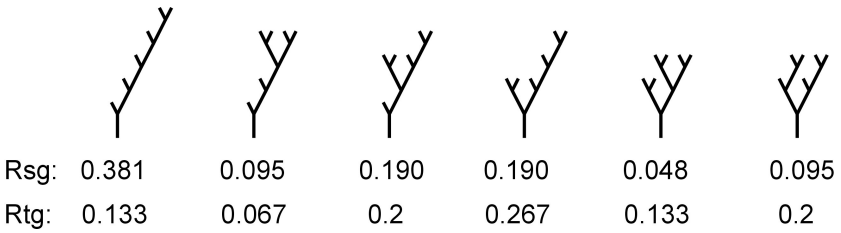

Figure 10.5
Probabilities of tree types grown with the random segmental growth (rsg) and the random terminal growth (rtg) mode of branching (Van Pelt and Verwer, 1983).

In an extensive study of experimental reconstructed motoneurons Dityatev et al. (1995) showed that the model, as simple as it is, successfully described the topological variability in a large variety of motoneuronal dendrites. Additionally, the analysis of reconstructed dendritic branching patterns has shown that their topological variation is consistent with the terminal branching mode, which is in agreement with the process of neurite outgrowth where growth cones at the neuritic tips are the sites of branching. The analysis of tree-type frequencies in terms of the mode of branching can be applied to other natural branching patterns as well, such as rivers systems. Where the branching process in river systems is more difficult to investigate, given the time scale of their development, the topological analysis suggested a process of terminal branching with a preference for the distal parts of the river as an alternative to the mostly studied random segmental growth mode (Van Pelt et al., 1989). This finding was a support for the headward network growth hypothesis, adopted by many geomorphologists.

Variation in the Number of Terminal Segments

The probability distribution of topological tree types has been obtained for a growth process with a given number of branching events. The occurrence of a branching event, however, is also stochastic, implicating that after a given time interval trees have been obtained with a varying number of terminal segments. For the calculation of the terminal segment number distribution in a population of trees, we will ignore the topological differentiation and label a tree only by its terminal segment number. This process requires a description in time with branching probabilities of segments defined as functions of time. In addition, we assume that the branching probability per unit of time of a terminal segment may depend on the momentary number of terminal segments in the growing tree. The stochastic nature of the branching process implicates that varying number of branching events occurs in a growing tree in a given time interval.

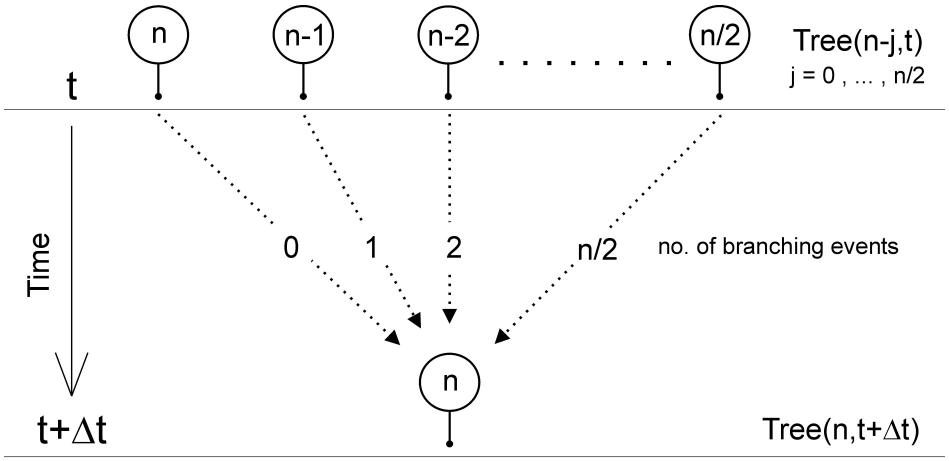

$$P_{tree}(n,t+\Delta t)=\sum_{j=0}^{n/2}P_{tree}(n-j,t)\cdot\binom{n-j}{j}\cdot[\bar{p}_s(t|n-j)\Delta t]^j\cdot[1-\bar{p}_s(t|n-j)\Delta t]^{n-2j}$$

Figure 10.6
Trees with *n* terminal segments may originate from trees of different size, dependent on the number of branching events per time interval.

This is illustrated in figure 10.6 showing that trees with different number of terminal segments at time t may give rise to trees with n terminal segments at time point $t + \Delta t$, dependent on the number of branching events in time period Δt. All these possibilities contribute to the probability of trees with n terminal segments at time *t*.

For the calculation of the distribution one needs to include all the possible growth sequences in a certain period of time. To this end Van Pelt and Uylings (2002) used the recurrent equation

$$P_{tree}(n,t+\Delta t)=\sum_{j=0}^{n/2}P_{tree}(n-j,t)\cdot\binom{n-j}{j}\cdot\left[\bar{p}_s(t\mid n-j)\Delta t\right]^j\cdot\left[\left(1-\bar{p}_s(t\mid n-j)\right)\Delta t\right]^{n-2j}$$

(10.1)

with $P_{tree}(n,t)$ the probability of having a tree with *n* terminal segments at time *t*, and $\bar{p}_s(t\mid n)$ denoting the probability of branching of a terminal segment, averaged over all *n* terminal segments in the tree. A tree with *n* terminal segments at time $t+\Delta t$ emerges when *j* branching events occur in time interval $[t,t+\Delta t]$ in a tree with *n-j* terminal segments. The recurrent equation expresses the probabilities of all these possible contributions from $j=0,\ldots,n/2$. The last two terms express the probability that, in a tree with *n-j* terminal segments, a number *j* of them will branch while the remaining *n-2j* terminal segments will not do so. The combinatorial coefficient $\binom{n-j}{j}$ expresses the number of possible ways of selecting *j* terminal segments from the existing *n-j* ones. Note that the probability distribution of trees with varying terminal segment numbers is normalized at each time point *t* and thus obeys $\sum_{n=1}^{n_{\max}}P_{tree}(n,t)=1,\ \forall t$ with $n_{\max}$ denoting the maximal possible terminal segment number at time *t*.

Finally, the branching probabilities of segments per unit of time need to be defined in order to solve the recurrent equation. Here, we make some explicit assumptions. All the tips of a dendritic tree are assumed to participate in the branching process. Each tip is assumed to

branch with a certain probability per unit of time that may change during the outgrowth process. The time-dependent branching probability of a tip is assumed to consist of a time-dependent baseline branching rate function $D(t)$, a term dependent on the total number of tips n^{-E} with a free parameter E, and a term dependent on the position of the tip $2^{-S\gamma}$ with γ denoting the number of segments on the path from the root to the segment (centrifugal order), and *S* indicating a free parameter (this dependency was already mentioned in the section on the topological variation). The choice for implementing n-dependency by the term n^{-E} was made for its simplicity, its modulatory power and attractive behavior at E=0, and at E=1 when, with 1/n, the branching probability becomes inversely related to the number of segments. Then, the total branching rate in a growing dendrite is independent of its increasing number of terminal segments.

The choice for implementing position dependency by the term $2^{-S\gamma}$ was inspired by the binary nature of the branching structure. its modulatory power and the attractive behavior at S=0, and at S=1, when $2^{-\gamma}$ illustrates the distribution of some conserved quantity over the segments at different centrifugal orders. These choices for the model structure have been made in order to investigate whether the position of a segment in the tree or the total number of segments influence the branching probability of the individual segments.

$$p_s(t \mid n, \gamma) = D(t) n^{-E} 2^{-S\gamma} / C(t) \tag{10.2}$$

The position dependent term $2^{-S\gamma}$ actually implements a particular branching scheme for the segments in a tree, defining the topological variation as is discussed and illustrated in the previous section and in figure 10.4. For S=0 the branching scheme becomes the random terminal mode of growth. The term *C(t)* normalizes at each point in (developmental) time the position-dependency of all tips. Then, the term $2^{-S\gamma} / C(t)$ only contributes to the topological variation and not to the growth rate of the tree (the increase in number of tips in the tree per unit of time). Thus, the mean branching probability of a terminal segment, averaged over all terminal segments is given by

$$\overline{p}_s(t \mid n) = \frac{1}{n} \sum_{i=1}^{n} D(t) n^{-E} 2^{-S\gamma} / C(t) = D(t) n^{-E} \tag{10.3}$$

Inserting this expression into equation (10.1) yields

$$P_{tree}(n, t+\Delta t) = \sum_{j=0}^{n/2} P_{tree}(n-j, t) \cdot \binom{n-j}{j} \cdot \left[D(t)(n-j)^{-E} \Delta t\right]^j \cdot \left[\left(1 - D(t)(n-j)^{-E} \Delta t\right)\right]^{n-2j}$$

(10.4)

Introducing the function $B(t) = \int D(t) dt$, with $dB(t) = D(t).dt$, and taking $\Delta B(t) = \frac{dB(t)}{dt} \Delta t = D(t).\Delta t$ we obtain

$$P_{tree}(n, t+\Delta t) = \sum_{j=0}^{n/2} P_{tree}(n-j, t) \cdot \binom{n-j}{j} \cdot \left[\Delta B(t)(n-j)^{-E}\right]^j \cdot \left[\left(1 - \Delta B(t)(n-j)^{-E}\right)\right]^{n-2j} .$$

(10.5)

Each iteration thus only depends on the value $\Delta B(t)$. For a given time period *T* and a given time step size Δt we have $N = T / \Delta t$ iterations, with the function $B(t)$ incrementing

with $\sum^{N} \Delta B(t) = B(T)$. For sufficiently small time steps Δt, the outcome of the iterations should not depend on the actual stepsize Δt but only on the sum of steps $\Delta B(t)$, thus on the value $B(T)$. This implicates that the terminal segment number distribution at time *t=T* is determined only by the function value *B(T)*, and not by the detailed shape of the function *D(t)*. The recursion can now be simplified by taking a number of N_c constant steps ΔB_c, such that $\sum^{N_c} \Delta B_c = B_c$ as

$$P_{tree}(n, t+\Delta t) = \sum_{j=0}^{n/2} P_{tree}(n-j, t) \cdot \binom{n-j}{j} \cdot \left[\Delta B_c (n-j)^{-E}\right]^j \cdot \left[\left(1 - \Delta B_c (n-j)^{-E}\right)\right]^{n-2j}, \quad (10.6)$$

with a time period associated with this number of iterations equal to $T_{B_c} = \sum^{N_c} \Delta t$.

An example of the family of distributions obtained for *B=6* and for several values of the parameter E is given in figure 10.7.

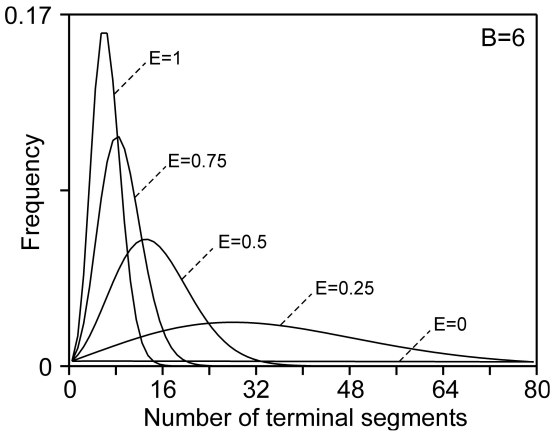

Figure 10.7
Frequency distributions of the terminal segment number of trees obtained for the parameter value *B=6* and for different values of the parameter *E*. Note, that the mean and the width of the curves (SD) decrease with increasing values of the parameter *E*. For E=0, the distribution gets an monotonically decreasing shape.

The curves in figure 10.7 show the effect of the parameter E on the shape of the terminal segment number distribution. The value *E=0* results in a monotonically decreasing function (with a long tail exceeding the size of the figure) while for positive values of *E* a modal shape is obtained with decreasing mean and standard deviation for increasing values of *E*. Actually a direct relation exist between the parameter pair (*B, E*) and the mean and standard deviation of the terminal segment number distributions, allowing a mapping of (*B, E*)-space onto (mean, SD)-space (Van Pelt et al., 1997). Empirical distributions of the terminal segment number do not show exponential shapes. They all have a clear modal shape, indicating that a zero value for parameter *E* is not realistic, but that *E* should be positive. For positive values of *E* the branching probability of a terminal segment decreases with increasing number of tips (equation 10.2), suggesting some competitive mechanism in the branching process.

Empirical distributions for the terminal segment number have been analysed for a number of different cell types. All these empirical distributions could be matched with model distributions by optimizing the values for the parameters *B* and *E* (Van Pelt et al., 1997). This is a remarkable result for a model that is based on only a few basic assumptions of the branching process. A scatter plot of the optimized parameter values in (*B,E*)-space showed a strong clustering per cell type, indicating that these values provide a significant characterization of cell types on the basis of the shape of their branching patterns (Van Ooyen and Van Pelt, 2002).

Growth Curves of the Number of Terminal Segments

During outgrowth the terminal segment number distribution in a population of dendrites will change with time reflecting in its mean and standard deviation the increase in the number of terminal segments. At each point in time the shape of the distribution is determined by the parameter values *B* and *E*, with *B* also a function of time ($B(t) = \int D(t)dt$). The growth of a population of dendrites thus can be calculated when the time course of the function *D(t)* is known. The function *D(t)*, however, is unknown and represents all factors influencing the growth process not covered by the dependence on the number of terminal segments. The function *D(t)* thus represents an essential determinant of the outgrowth process.

Van Pelt and Uylings (2002) calculated dendritic growth curves for different choices of the function *D(t)*. It was shown that a constant function *D(t)* resulted in an exponentially increasing growth curve while an exponential decreasing function $D(t) = ce^{-t/\tau}$ resulted in an asymptotic shape for the growth curve. Experimental data on the growth of the mean number of terminal segments in populations of dendrites at different time points during development did not showed an exponential growth pattern. In fact, the experimental data was in good agreement with the growth curve predicted by the exponential decreasing function *D(t)*. These results indicate that the baseline branching rate function *D(t),* representing the basic drive for branching of a neuron is not constant but rapidly decreasing with time elapsing from the start of outgrowth (Fig. 10.8).

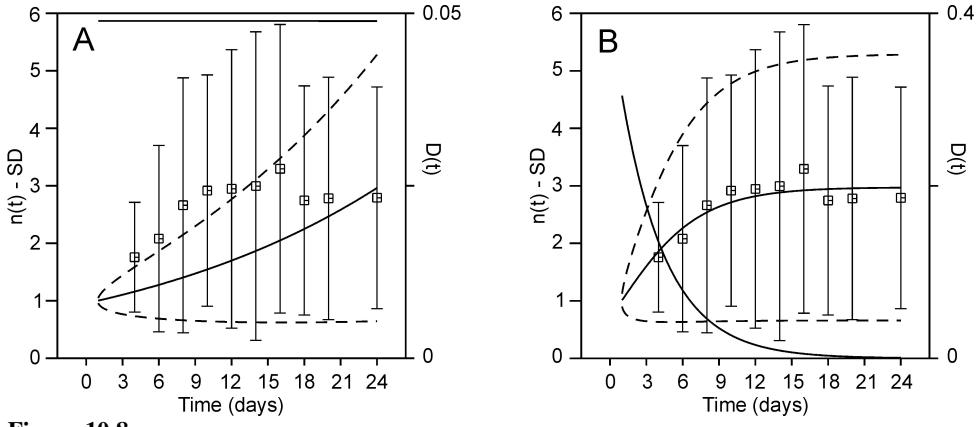

Figure 10.8

Growth curves of the population mean and standard deviation (SD) of the terminal segment number in dendritic trees during their outgrowth (Van Pelt and Uylings, 2002). The data points and SD bars originate from reconstructed dendrites of rat cortical multipolar nonpyramidal cells at several time points during their development (Parnavelas and Uylings, 1980; Uylings et al, 1980). The model growth curves (continuous curve for the mean and dashed lines for the SD-values) are calculated for parameter values *E=0.05*, *B=1.12*, and assuming for panel (A) a constant baseline branching rate function (see horizontal line in top of panel), and panel (B) an exponential decreasing baseline branching rate function $D(t) = ce^{-t/\tau}$ with $\tau = 3.7d$. With the latter choice an excellent agreement is obtained between model predictions and experimental data both in the time course of the mean but also of the SD values. Left ordinate scale refer to the number of terminal segments. Right ordinate scale refers to the baseline branching rate function.

From the recursion in equation (10.1), an expression can be derived for the time pattern of the mean number of terminal segments per tree $\overline{n}(t)$, averaged over the population of trees, as $\frac{d\overline{n}(t)}{dt} = D(t)\overline{n^{1-E}}(t)$ (publication in preparation). In previous studies we have investigated the growth equation $\frac{dn(t)}{dt} = D(t)n(t)^{1-E}$ for the growth of a virtual tree with a real variable $n(t)$ for its number of terminal segments. In this equation the discrete process of adding integer numbers of terminal segments per growth step has been changed into a continuous process of adding infinitesimal values to a virtual number of terminal segments. The growth pattern of the virtual tree coincides with the population mean for the parameter values *E=0* or *E=1*.

The accuracy with which the growth function of the virtual tree approximates the population mean growth function for other values of the parameter *E* is presently under study. The analytical treatability of the virtual tree growth function made it possible to investigate quantitatively the effect of different baseline branching rate functions on the virtual tree growth patterns (Van Pelt and Uylings, 2002; 2003). These studies showed that even decreasing power functions for the baseline branching rate were not able to suppress the growth rate of the tree to zero values. Indeed, exponential functions were able to compensate the proliferation of branching segments and force the tree growth rate to zero values, and terminating the growth phase.

Neurite Elongation

The lengths of segments in a dendritic tree are determined by both the branching rates and the elongation rates of neurites. The distribution of segment lengths in a tree, and its developmental changes with time, is thus the outcome of a complex integrated process of branching and elongation rates during development. So far we have dealt with the branching process and we were able to derive quantitative details in terms of baseline branching rate functions and size dependencies from experimental dendritic reconstructions. This approach thus also holds promises for the challenge to derive quantitative details of the elongation process, using these model-based approaches.

In a recent study a first attempt was made to estimate elongation rates from an experimental data set of rat multipolar nonpyramidal neurons (Van Pelt and Uylings, 2003). In particular the question was addressed whether elongation rates were constant during the growth of a dendrite or would reflect competitive effects because of the proliferation of elongating neurites. The elongation rate is assumed to depend on the number of terminal segments $v(t) = v_0 n(t)^{-F}$, with v_0 denoting the elongation rate of the initial segment at the start of the branching process, and with a dependence on the number of terminal segments modulated by the exponent *F*. Using the virtual tree growth function for this segment number, an estimate could be formulated for the total tree length growth function,

$$L(t) = L_0 + v_0 \int_{t_0}^{t} \left[1 + EB_\infty \left(1 - e^{-(s-t_0)/\tau}\right)\right]^{(1-F)/E} ds$$

(Van Pelt and Uylings, 2003), with L_0 denoting the initial length of daughter branches after a branching event. Comparison with the observed growth function suggested a small competitive effect in the elongation rate (figure 10.9). These rat multipolar nonpyramidal dendritic trees are, however, small with on the average about three terminal segments per dendrite. Developmental data sets of larger trees are therefore required to show more clearly any possible competitive effect in the elongation rate.

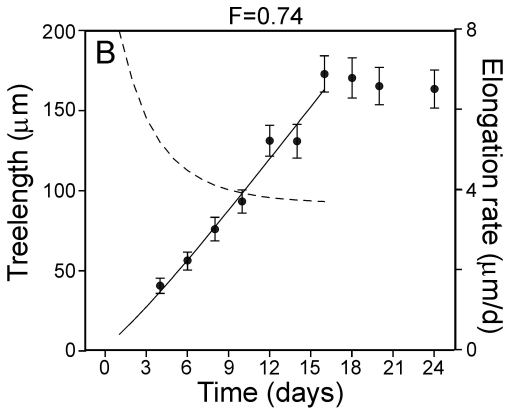

Figure 10.9
Mean and SEM (data points) of the total length of dendritic trees of rat cortical multipolar nonpyramidal cells at several time points during development (Parnavelas and Uylings, 1980; Uylings et al, 1980). The tree length growth function (solid line) has been obtained using the optimized parameter values for the branching process and by fitting the tree growth length function to the data points, resulting in optimized parameter values $L_0 = 10$ μm, $F = 0.73$ and $v_0 = 8.1$ μm/day (Van Pelt and Uylings, 2003). The corresponding elongation rate function $v(t) = v_0 n(t)^{-F}$ is shown as a dashed line.

The model-based analysis of segment length distributions has also focused the attention on the elongation process during and following a branching event. When a branching event is a point process in time, and the daughter branches immediately continue their outgrowth, one expect a monotonous decreasing length distribution with the highest probabilities for the shortest segments figure 10.10A.

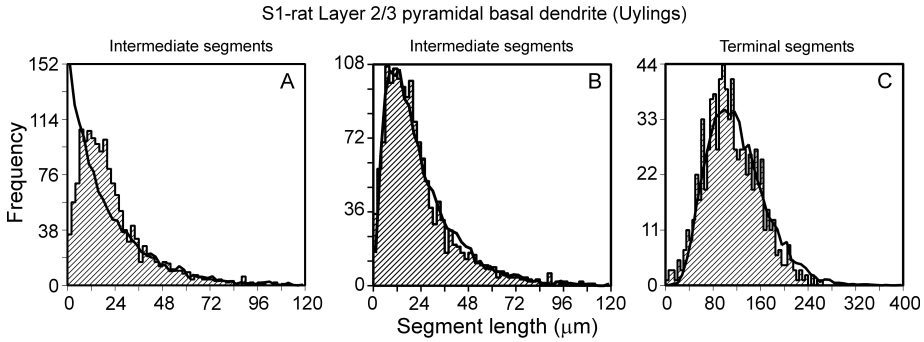

Figure 10.10
Segment lengths distributions in S1-rat cortical layer 2/3 pyramidal cell basal dendrites (Uylings et al., 1994) of intermediate segments (A and B, plotted with different scales) and terminal segments (C). Model predictions obtained for optimized parameter values without (A) and with (B, C) initial lengths of daughter segments after a branching event (Van Pelt et al., 2001).

Observed segment length distributions, however, have a modal shape in contrast to these expectations. To answer this question it is important to realize that in the model the branching process is reduced to a point process both in time and in space. A biological growth cone, however, has a spatial extent, while its branching proceeds during a certain period in time. To solve this problem we have assumed that after a branching event in the model the daughter branches already appear with a certain initial length (figure 10.11), resulting in a model length distribution closely matching the observed one (figure 10.10B). Nowakowski et al. (1992), alternatively, assumed in their model description a transient reduction in the branching

probability. Both approaches resulted in a good description of the intermediate segment length distribution.

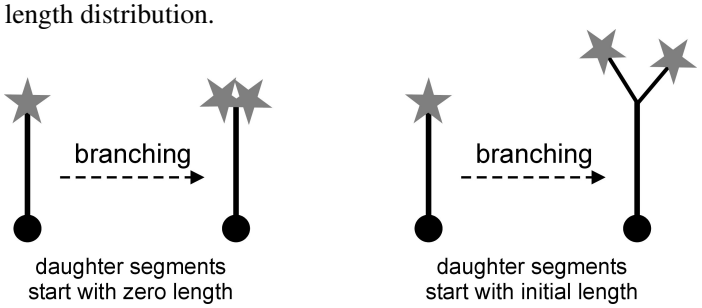

Figure 10.11
Schematic view of the initial length assumption of daughter segments after a branching event to comply with the non-infinitesimal character of branching events in space-time.

Terminal segments are generally longer than intermediate ones, as also shown in figure 10.10B and 10.10C. This may occur, for instance, when dendritic development proceeds in two different phases, the first one showing neurites to branch and elongate, followed by a second phase with neuritic elongation only, as is the case in rat pyramidal cell basal dendrites. Assuming different elongation rates during both phases, the observed segment length distributions could accurately be reproduced for these cell types. Even with constant elongation rates during dendritic development, changing branching rates will influence segment length distributions in dendritic trees in a complex, nontrivial way. For studying these questions a good description of the branching process is required. Therefore, we are now at the beginning of quantitative exploration of the elongation rates, with the distributions of observed dendritic shape parameters as a wealthy source of information.

Variability in the Shape of Dendritic Trees
An impression of the shape properties and variability is given in figure 10.12, illustrating a population of model generated dendrograms reflecting the properties of cat deep layer superior colliculus neurons (Van Pelt et al., 2001). The examples show the variation in the number of terminal segments per tree and in the length of both intermediate and terminal segments. Segment diameters have been assigned to the segments according to the following rule. Terminal segments are first assigned a mean diameter of 1.05 μm, followed by the calculation of the diameter of a parent segment d_p from the diameters of its daughters d_1 and d_2 using the branch power rule $d_p^e = d_1^e + d_2^e$, with the branch power e randomly sampled from a normal distribution with mean=1.47 and SD=0.3 (Schierwagen and Grantyn, 1986) .

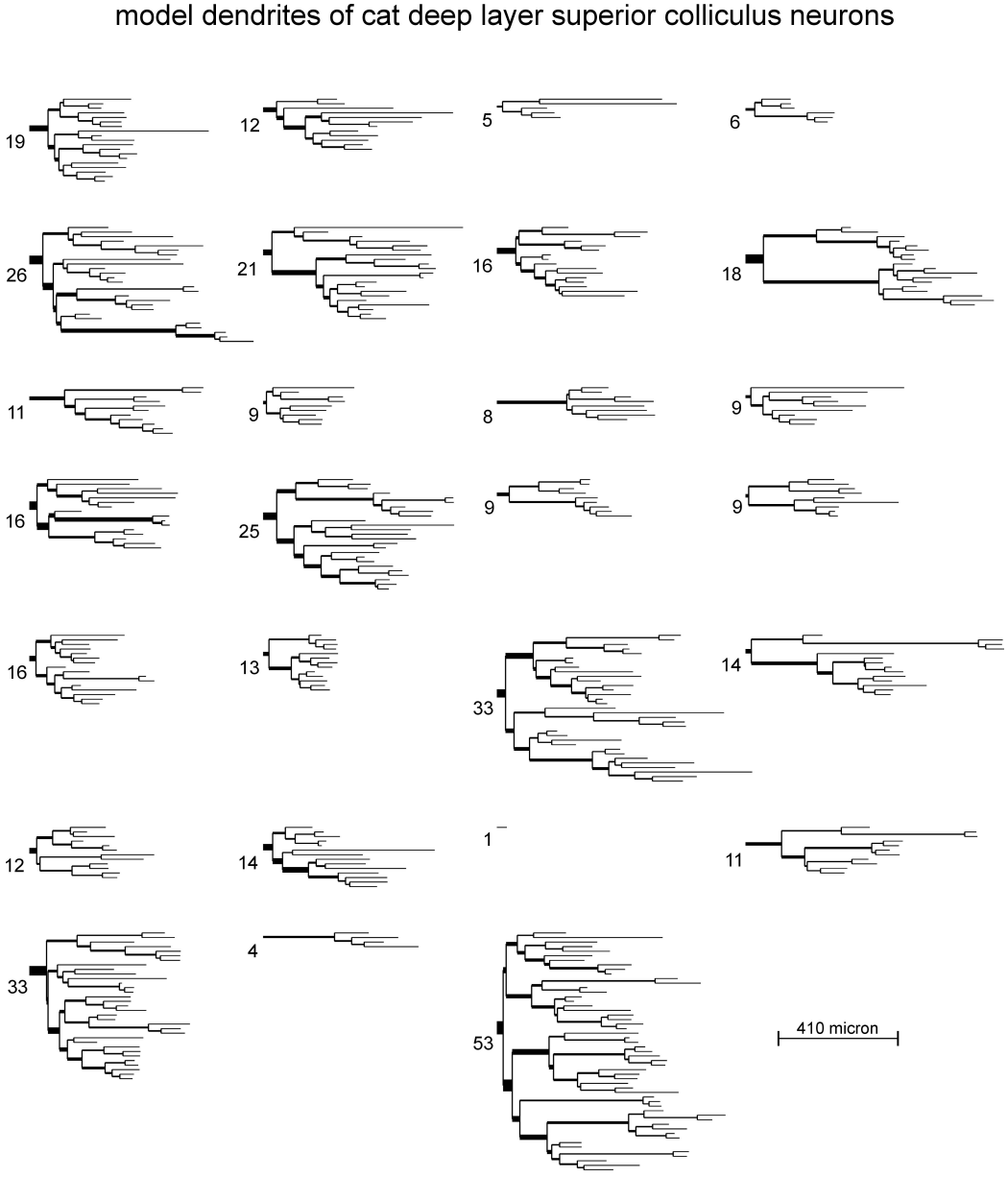

Figure 10.12
Illustration of morphological variability in a set of model dendrites generated using parameter values optimized for dendrites of cat superior colliculus neurons (Schierwagen and Grantyn, 1986; Van Pelt et al., 2001). Variability is shown in the number, the length and the connectivity pattern of the segments. Terminal segment diameters have been randomly drawn from a normal distribution. Parent segments have been assigned a diameter using a power law relation with the daughter segment diameters, with a branch power randomly drawn from a normal distribution (see text). The number of terminal segments of each tree is indicated at the root of the tree.

Conclusion

Mathematical modeling contributes significantly to the understanding and the quantitative description of biological structures and processes. This has been illustrated in this chapter for the shape and variability of dendritic branching patterns. The modeling approach has demonstrated that (i) randomness in elongation and branching is sufficient to explain the variability in the ultimate shapes, (ii) the branching probability depends on the momentary number of terminal segments in the growing tree, and (iii) the branching probability depends

on an intrinsic component (basal branching rate function) that rapidly (as strong as exponentially) decreases with time of development. Ongoing studies of segment length distributions are expected to clarify whether neurite elongation rates are also subjected to competitive influences due to the proliferation of the number of segments in the growing tree. For these modeling studies dendritic shape complexity was reduced down to skeleton trees maintaining segment number, segment length and segment connectivity (topology).

The conclusions from these modeling studies need to be followed by experimental investigations for the cell biological mechanisms underlying the basal branching rate and the dependencies on the number of terminal segments. Clearly, the modeling approach was essential to unravel the influence of the branching and elongation processes on the segment length structure in dendritic trees.

References

Acebes A, Ferrus A (2000) Cellular and molecular features of axon collaterals and dendrites. Trends Neurosci. 23: 557-565.

Ascoli GA, Krichmar JL, Scorcioni R, Nasuto SJ, Senft SL (2001) Computer generation and quantitative morphometric analysis of virtual neurons. Anat Embryol 204: 283-301.

Ascoli GA (2002a) Neuroanatomical algorithms for dendritic modeling. Network: Computation in Neural Systems 13: 247-260.

Ascoli GA (2002b) Computational Neuroanatomy – Principles and Methods, Ascoli, GA (ed). Humana Press, Totowa, New Jersey.

Berry M, Bradley P (1976a) The growth of the dendritic trees of Purkinje cells in the cerebellum of the rat. Brain Res. 112: 1-35.

Berry M, Bradley PM (1976b) The application of network analysis to the study of branching patterns of large dendritic fields. Brain Res. 109: 111-132.

Black MM (1994) Microtubule transport and assembly cooperate to generate the microtubule array of growing axons. In The Self-Organizing Brain: From Growth Cones to Functional Networks, Van Pelt, J, Corner, MA, Uylings, HBM, Lopes da Silva, FH (eds), Progress in Brain Research, Vol 102, pp. 61-77. Elsevier, Amsterdam.

Carriquiry AL, Ireland WP, Kliemann W, Uemura E (1991) Statistical evaluations of dendritic growth models. Bull. Math. Biol. 53, 579-589.

Cline H.T. (1999) Development of dendrites. In: Dendrites, Stuart, G, Spruston, N, Hausser, M (eds), Oxford Un. Press, 1999, pp35-56.

Costa LF, Manoel ETM, Faucereau F, Chelly J, Van Pelt J, Ramakers G (2002) A shape analysis framework for neuromorphomery. Network: Comput. Neural Syst. 13: 283-310.

Dityatev AE, Chmykhova NM, Studer L, Karamian OA, Kozhanov VM, Clamann HP (1995) Comparison of the topology and growth rules of motoneuronal dendrites. J. Comp. Neurol. 363: 505-516.

Horsfield K, Woldenberg MJ, Bowes CL (1987) Sequential and synchronous growth models related to vertex analysis and branching ratios. Bull. Math. Biol. 49: 413-430.

Ireland W, Heidel J, Uemura E (1985) A mathematical model for the growth of dendritic trees. Neurosc. Lett. 54: 243-249.

Kater SB, Davenport RW, Guthrie PB (1994) Filopodia as detectors of environmental cues: signal integration through changes in growth cone calcium levels. In The Self-Organizing Brain: From Growth Cones to Functional Networks, Van Pelt, J, Corner, MA, Uylings, HBM, Lopes da Silva, FH (eds) Progress in Brain Research, Vol 102, pp. 49-60. Elsevier, Amsterdam.

Kater SB, Rehder V 1995) The sensory-motor role of growth cone filopodia. Current Opinion in Neurobiology 5:68-74.

Kliemann WA (1987) Stochastic dynamic model for the characterization of the geometrical structure of dendritic processes. Bull. Math. Biol. 49:135-152.

Larkman A, Mason A (1990) Correlations between morphology and electrophysiology of pyramidal neurons in slices of rat visual cortex. I. Establishment of cell classes. J. Neurosci. 10: 1407-1414.

Letourneau PC, Snow DM and Gomez TM (1994) Growth cone motility: substratum-bound molecules, cytoplasmic [Ca^{2+}] and Ca^{2+}-regulated proteins. In The Self-Organizing Brain: From Growth Cones to Functional Networks, Van Pelt, J, Corner, MA, Uylings, HBM, Lopes da Silva, FH (eds) Progress in Brain Research, Vol 102, pp. 35-48. Elsevier, Amsterdam.

Mason A, Larkman A (1990) Correlations between morphology and electrophysiology of pyramidal neurons in slices of rat visual cortex. II. Electrophysiology. J. Neurosc. 10: 1415-1428.

McAllister AK (2002) Conserved cues for axon and dendritic growth in the developing cortex. Neuron 33: 2-4.

Nowakowski RS, Hayes NL, Egger MD (1992) Competitive interactions during dendritic growth: a simple stochastic growth algorithm, Brain Res. 576: 152.

Ramakers GJA, Avci B, Van Hulten P, Van Ooyen A, Van Pelt J, Pool CW, Lequin MB (2001) The role of calcium signaling in early axonal and dendritic morphogenesis of rat cerebral cortex neurons under non-stimulated growth conditions. Dev. Brain Res. 126: 163-172.

Ramakers GJA, Winter J, Hoogland TM, Lequin MB, Van Hulten P, Van Pelt J, Pool CW (1998) Depolarization stimulates lamellipodia formation and axonal but not dendritic branching in cultured rat cerebral cortex neurons. Dev. Brain Res. 108: 205-216.

Schierwagen A, Grantyn R (1986) Quantitative morphological analysis of deep superior colliculus neurons stained intracellularly with HRP in the cat. J Hirnforsch 27: 611-623

Schierwagen A (1986) Segmental cable modeling of electrotonic transfer properties of deep superior colliculus neurons in the cat. J. Hirnforsch. 27: 679-690.

Scorcioni R, Lazarewicz MT, Ascoli GA (2004) Quantitative morphometry of hippocampal pyramidal cells: differences between anatomical classes and reconstructing laboratories. J. Comp. Neurol. 473: 177-193.

Smit GJ, Uylings HBM, Veldmaat-Wansink L (1972) The branching pattern in dendrites of cortical neurons. Acta Morphol. Neerl.-Scand. 9: 253-274.

Song HJ, Poo MM (2001) The cell biology of neuronal navigation. Nature Cell Biology 3: E81-E88.

Tamori Y (1993) Theory of dendritic morphology. Physical Review E 148: 3124-3129.

Uemura E, Carriquiry A, Kliemann W, Goodwin J (1995) Mathematical modeling of dendritic growth in vitro. Brain Research 671: 187-194.

Uhlfhake B, Cullheim S (1988) Postnatal development of cat hind limb motoneurons. II: In vivo morphology of dendritic growth cones and the maturation of dendrite morphology. J. Comp. Neurol. 278: 88-102.

Uylings HBM (2000) Development of the cerebral cortex in rodents and man. Eur. J. Morphol. 38: 309-312.

Uylings HBM, Van Pelt J (2002) Measures for quantifying dendritic arborizations. Network: Comput. Neural Syst. 13: 397-414.

Van Ooyen A, Willshaw DJ (1999) Competition for neurotrophic factor in the development of nerve connections. Proc. R. Soc. Lond. B 266: 883-892.

Van Ooyen A, Willshaw DJ (2000) Development of nerve connections under the control of neurotrophic factors: parallels with consumer-resource systems in population biology. J. Theor. Biol. 206: 195-210.

Van Ooyen A (2001) Competition in the development of nerve connections: a review of models. Network: Comput. Neural Syst. 12: R1-R47.

Van Ooyen A, Van Pelt J. (2002) Competition in neuronal morphogenesis and the development of nerve connections. In: Computational Neuroanatomy: Principles and Methods, G. Ascoli (ed.), The Humana Press Inc, Totowa, NJ, pp. 219-244.

Van Pelt J, Verwer RWH (1983) The exact probabilities of branching patterns under segmental and terminal growth hypotheses. Bull. Math. Biol. 45: 269-285.

Van Pelt J, Verwer RWH (1986) Topological properties of binary trees grown with order-dependent branching probabilities. Bull. Math. Biol. 48: 197-211.

Van Pelt J, Woldenberg MJ, Verwer RWH (1989) Two generalized topological models of stream network growth. J. Geol. 97: 281-299.

Van Pelt J, Dityatev AE, Uylings HBM (1997) Natural variability in the number of dendritic segments: Model-based inferences about branching during neurite outgrowth. J. Comp. Neurol. 387: 325-340.

Van Pelt J, Schierwagen A, Uylings HBM (2001) Modeling dendritic morphological complexity of deep layer cat superior colliculus neurons. Neurocomputing 38-40: 403-408.

Van Pelt J, Van Ooyen A, Uylings HBM (2001) Modeling dendritic geometry and the development of nerve connections. In: Computational Neuroscience: Realistic modeling for experimentalist, De Schutter, E (ed) and Cannon, RC (CD-ROM)), CRC Press, Boca Raton, pp.179-208.

Van Pelt J, Uylings HBM (2002) Branching rates and growth functions in the outgrowth of dendritic branching patterns. Network: Comput. Neural Syst. 13: 261-281.

Van Pelt J, Uylings HBM (2003) Growth functions in dendritic outgrowth. Brain and Mind 4: 51-65.

Whitford KL, Marillat V, Stein EW, Goodman CS, Tessier-Lavigne M, Chedotal A, Ghosh A (2002) Regulation of cortical dendrite development by slit-robo interactions. Neuron 33: 47-61.

Zhang LI, Poo MM (2001) Electrical activity and development of neural circuits. Nature Neurosci. 4 Suppl: 1207-14.